

# Quantum-Coherent Thermodynamics: Leaf Typicality via Minimum-Variance Foliation

Maurizio Fagotti<sup>1,\*</sup>

<sup>1</sup>Université Paris-Saclay, CNRS, Laboratoire de Physique Théorique et Modèles Statistiques, 91405, Orsay Cedex, France.

Equilibrium statistical ensembles commute with the Hamiltonian and thus carry no coherence in the energy eigenbasis. We develop a thermodynamic framework in which energy fluctuations can retain genuinely quantum-coherent contributions. We foliate state space into “minimum-variance leaves,” defined by minimizing the average energy variance over all pure-state decompositions, with the minimum set by the quantum Fisher information. On each leaf we construct the least-biased state compatible with normalization and mean energy, defining a leaf-canonical ensemble. The Gibbs ensemble is recovered on the distinguished commuting leaf, while generic states are organized by their leaf label. This structure provides a natural setting to extend eigenstate thermalization beyond equilibrium via a “leaf typicality” hypothesis. According to that hypothesis, under unitary time evolution local observables depend only on the leaf and energy and, at all times, are reproduced by evolving a representative (pure) state drawn from the optimal ensemble.

*Introduction.* Many-body quantum systems quickly exceed the reach of fully microscopic analysis, and even when such analyses are possible, their implications are most naturally read through thermodynamic lenses. Statistical mechanics enables this by distilling microscopic complexity into a tractable set of macroscopic properties that govern accessible observables. This reduction is particularly effective at equilibrium, whereas constructing an equally systematic and efficient framework out of equilibrium has been a long-standing objective since the origins of statistical mechanics [1]. A central question in nonequilibrium many-body physics is how relaxation to equilibrium occurs, and what notion of equilibration is appropriate [2–5]. This has encouraged the view that thermodynamic descriptions are, by construction, late-time descriptions.

In this Letter, we challenge that association and adopt a different point of view. To clarify the shift in perspective, it is useful to recall an analogous development in quantum measurement theory. In the traditional von Neumann formulation, measurements were identified with projections (collapses) onto the eigenstates of the measured observable. Let the observable be  $H$  and, for simplicity, assume that it is nondegenerate with eigenstates  $\{|\varphi_i\rangle\}$ . If one performs a projective measurement of  $H$  and ignores the outcome, the post-measurement state commutes with  $H$  and takes the diagonal form

$$\rho[\{p\}] = \sum_i p_i |\varphi_i\rangle \langle \varphi_i|, \quad (1)$$

where  $p_i$  are the outcome probabilities. The connection with equilibrium thermodynamics is that, when  $H$  is interpreted as the Hamiltonian, this class of states contains canonical (Gibbs) ensembles. Ultimately, however, the elegance of projective measurements is an idealization: in practice measurements are typically indirect or sequential, motivating the development of generalized measurements [6]. Reinterpreting Eq. (1) in this spirit, one recognizes that moving from projective to positive

operator-valued measurements amounts to relaxing the orthogonality of the post-measurement ensemble  $\{|\varphi_i\rangle\}$ .

We propose to generalize thermodynamic ensembles in an analogous way. In our formulation, equilibrium ensembles will be special because the state carries no coherence in the energy eigenbasis: an equilibrium density matrix satisfies  $[\rho, H] = 0$  and is therefore insensitive to the unitary flow generated by  $H$ . Indeed, its quantum Fisher information [7, 8] with respect to  $H$  vanishes,  $F_Q(\rho; H) = 0$ . Out of equilibrium, this condition is not met, and the traditional perspective is naturally focussed on dynamical mechanisms, such as dephasing [9–12], that suppress energy-basis coherence and, in turn, drive  $F_Q(\rho(t); H)$  towards zero at late times. The appeal of equilibration lies in its drastic reduction of complexity: once equilibrium is reached, statistical mechanics suggests that microscopic details become largely irrelevant and that the state is described by a small set of thermodynamic parameters (e.g., by a canonical ensemble). This viewpoint culminates in the eigenstate thermalization hypothesis [13–16], which asserts that, for generic nonintegrable systems, individual energy eigenstates are locally indistinguishable from the corresponding thermal ensemble: local observables depend essentially only on the energy density of the stationary state. Is this “thermodynamic paradise” really restricted to equilibrium?

*Coherent energy fluctuations.* Relaxing the assumption that ensemble states are stationary requires a shift of principle. Away from equilibrium, one gives up the criterion that singles out the “privileged” states underlying standard ensembles (the energy eigenstates), which are expected to capture the late-time local properties of broad classes of initial states (e.g., with clustering properties) [13–17]. We nevertheless aim at a statistical description of local physics that retains large equivalence classes of locally indistinguishable states (cf. the equivalence between microcanonical and canonical ensembles [18]). In this respect, controlling fluctuations remains a key implicit requirement for ensemble equivalence (cf. Refs. [19–

[\[21\]](#)). We make this requirement explicit and promote it to a principle of *minimal coherent energy fluctuations*. To this end, we single out families of pure states  $\{|\varphi_i\rangle\}$  (generally nonorthogonal) with the following property:

*For every choice of probabilities  $\{p_i\}$ , the density matrix  $\rho = \sum_i p_i |\varphi_i\rangle\langle\varphi_i|$  minimizes the ensemble-averaged energy variance among all pure-state decompositions of  $\rho$ .* In other words, for all  $\{p_i\}$  one has

$$\sum_i p_i \text{Var}_{\varphi_i}(H) = \inf_{\rho = \sum_j p'_j |\psi_j\rangle\langle\psi_j|} \sum_j p'_j \text{Var}_{\psi_j}(H) \quad (2)$$

$$\text{Var}_{\psi}(H) := \langle\psi|H^2|\psi\rangle - \langle\psi|H|\psi\rangle^2.$$

It is well known [\[22, 23\]](#) that the minimal average energy variance (over all pure-state decompositions) is directly related to the quantum Fisher information of  $\rho$  with respect to  $H$  [\[24\]](#). What is less appreciated (notwithstanding being a simple consequence of convexity) is that the same decomposition remains optimal for any convex combination of the states of the family  $\{|\varphi_i\rangle\}$  [\[25, 26\]](#), which consists of a number of states equal to the rank of  $\rho$ . In more mathematical terms, the minimal-variance decompositions induce a foliation of (a dense open subset of) the state space, with each leaf associated with a fixed family of pure states [\[25\]](#).

Following Yu [\[23\]](#), we define an effective “state Hamiltonian”  $H_\rho$  (called  $Y$  in Ref. [\[23\]](#)) as the operator satisfying

$$\frac{1}{2}\{H_\rho, \rho\} = \rho^{\frac{1}{2}} H \rho^{\frac{1}{2}}. \quad (3)$$

This operator reduces to  $H$  if  $\rho$  commutes with  $H$ . In addition,  $H_\rho$  has the same expectation value of  $H$ . Ref. [\[23\]](#) showed that the optimal ensemble and the populations are directly related to the eigenvectors,  $|\Psi_i\rangle$ , and eigenvalues,  $E_{\rho,i}$ , of  $H_\rho$ ,  $H_\rho |\Psi_i\rangle = E_{\rho,i} |\Psi_i\rangle$ , as follows

$$\begin{aligned} p_i &= \langle\Psi_i|\rho|\Psi_i\rangle \\ |\varphi_i\rangle\langle\varphi_i| &= \frac{1}{p_i} \sqrt{\rho} |\Psi_i\rangle\langle\Psi_i| \sqrt{\rho} \\ \langle\varphi_i|H|\varphi_i\rangle &= E_{\rho,i}. \end{aligned} \quad (4)$$

As argued by Yu, this implies that the decomposition is unique if  $H_\rho$  is nondegenerate.

*Leaf canonical ensemble.* From (4) it readily follows that, if  $\rho$  has full rank, any other density matrix in the same leaf (i.e. obtained by varying the populations while keeping the same optimal family) can be written as

$$\rho' = \frac{\sqrt{\rho} R_H^{(\rho)} \sqrt{\rho}}{\text{tr}[\rho R_H^{(\rho)}]}, \quad R_H^{(\rho)} \geq 0, \quad [R_H^{(\rho)}, H_\rho] = 0. \quad (5)$$

In analogy with the Gibbs–Jaynes maximum-entropy prescription [\[27\]](#), we define the *min-variance leaf canonical ensemble* by maximizing the Shannon entropy of the populations,  $S_H[\rho] = -\sum_i p_i \log p_i$ , subject to normaliza-

tion and fixed mean energy. Since  $\{E_\rho^{(i)}\}$  are independent of  $\{p_i\}$  and within a given leaf the energy reads

$$E[\rho] = \sum_i p_i \langle\varphi_i|H|\varphi_i\rangle = \sum_i p_i E_{\rho,i}, \quad (6)$$

the maximization yields the usual Gibbs weights  $p_i \propto e^{-\beta E_\rho^{(i)}}$ . This strong analogy leads us to identify  $S_H[\rho]$  with the nonequilibrium generalization of the thermodynamic entropy. More explicitly, it is convenient to consider the reference density matrix  $\rho_0$  with uniform weights (equal to the inverse of the dimension of the Hilbert space), which we dub “barycentre of the leaf”. Then, the associated min-variance leaf canonical ensemble reads

$$\rho_{\beta|\mathcal{L}_H(\rho_0)} = \frac{\sqrt{\rho_0} \exp(-\beta H_{\rho_0}) \sqrt{\rho_0}}{\text{tr}[\rho_0 \exp(-\beta H_{\rho_0})]}, \quad (7)$$

where  $\mathcal{L}_H(\rho_0)$  denotes the leaf through  $\rho_0$ . Just as the Gibbs ensemble provides the canonical effective description obtained by discarding microscopic information beyond the mean-energy constraint within the equilibrium paradigm, the leaf-canonical ensemble arises once the leaf is specified. That is to say, one fixes the leaf label (i.e., the relevant min-variance family) and then selects, within that leaf, the least biased state consistent with normalization and energy. Standard equilibrium is recovered as the special case where the state is restricted to the commuting leaf,  $[\rho, H] = 0$ , which corresponds to  $\rho_0 \propto \mathbf{I}$ . Analogously, we define a leaf-microcanonical ensemble by replacing  $\exp(-\beta H_{\rho_0})$  in Eq. (7) with the projector onto the chosen energy shell of  $H_\rho$ , and then normalizing.

We remark that a genuine foliation requires leaves to be pairwise disjoint. This fails on the full state space: at points where  $H_\rho$  is degenerate the (variance) minimizing ensemble is not unique, and distinct leaves meet. It does, however, hold on the open subset  $\mathcal{M}_H := \{\rho : H_\rho \text{ is nondegenerate}\}$ , where the minimizing family of pure states is uniquely determined [\[23\]](#) (up to phases and permutation) and therefore labels a single leaf. Whenever we speak of a foliation we implicitly restrict to  $\mathcal{M}_H$ . For a generic choice of  $H$  (in particular, after lifting accidental degeneracies),  $\mathcal{M}_H$  is open and dense in the space of density matrices.

*Quantifying energy (in)coherence.* This foliation provides a concrete handle on quantum coherence with respect to  $H$ , i.e., coherence in the energy eigenbasis [\[28, 29\]](#). The variance-minimizing optimal family  $\{|\varphi_i\rangle\}$  encodes the coherent structure, while varying the populations  $\{p_i\}$  amounts to classical mixing within that structure. The commuting leaf plays the role of an incoherent sector [\[30\]](#), in which the optimal family coincides with the energy eigenbasis and is orthonormal. Conversely, on the full-rank domain considered here, an orthonormal optimal family occurs only on the commuting leaf; thus, coherence across energy levels is faithfully witnessed by the nonorthogonality of  $\{|\varphi_i\rangle\}$ . A natural leaf-level incoherence indicator is provided by the barycenter

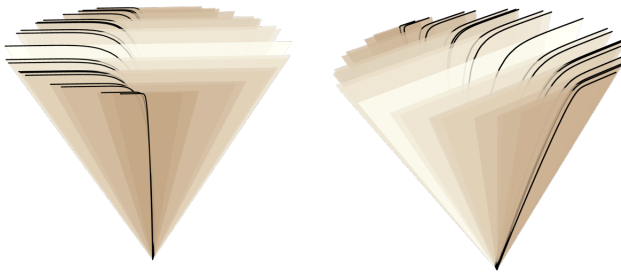


Figure 1. Representation of the foliation of the state space of a single spin-1, viewed from two angles. The subspace is constrained by the condition  $\text{tr}[\rho\lambda_j] = 0$  for  $j \in \{2, 4, 5, 6, 7\}$ , with Hamiltonian given by  $H = \frac{1}{2}\lambda_3 + \frac{3}{2}\sqrt{3}\lambda_8$ . The colors encode the degree of incoherence: the lightest yellow triangle marks the commuting leaf, while progressively darker (brown) shades correspond to increasing quantum coherence. Black curves represent the corresponding leaf-canonical ensembles, interpolating between the pure state at  $\beta \rightarrow -\infty$  and the pure state at  $\beta \rightarrow \infty$ .

$\rho_0(\mathcal{L}) := \frac{1}{d} \sum_{i=1}^d |\varphi_i\rangle \langle \varphi_i|$ , and its von Neumann entropy,  $\mathfrak{I}(\mathcal{L}) := S[\rho_0(\mathcal{L})] = -\text{tr}[\rho_0(\mathcal{L}) \log \rho_0(\mathcal{L})]$ . This is reminiscent of quantifiers of “ensemble quantumness” based on overlaps [31–33]. It satisfies  $0 \leq \mathfrak{I}(\mathcal{L}) \leq \log d$ , and it is maximal,  $\mathfrak{I}(\mathcal{L}) = \log d$ , if and only if  $\rho_0(\mathcal{L}) = \mathbf{I}/d$ , which occurs precisely on the commuting leaf. At the opposite extreme,  $\mathfrak{I}(\mathcal{L})$  can become arbitrarily small when the optimal states  $\{|\varphi_i\rangle\}$  become nearly collinear and  $\rho_0(\mathcal{L})$  approaches a pure state. Finally, we note that  $\exp[\mathfrak{I}(\mathcal{L})]$  can be interpreted as an effective measure of the state-space volume associated with that leaf.

*Examples.* For a single spin- $\frac{1}{2}$ , the min-variance foliation admits a simple geometric picture. Without loss of generality we set  $H = \varepsilon\sigma^z$  and represent states as points in the Bloch ball,  $\rho = \frac{1}{2}(\mathbf{I} + \vec{r} \cdot \vec{\sigma})$  with  $|\vec{r}| \leq 1$ . The leaves are the straight chords parallel to the  $z$  axis: each leaf is specified by a fixed transverse component  $\vec{r}_\perp = \vec{r} - (\vec{r} \cdot \hat{z})\hat{z}$ , while the population parameter moves the state along  $z$ . The two pure states at the endpoints of a leaf have Bloch vectors  $\hat{n}$  and its reflection through the  $xy$ -plane,  $\hat{n}' = \hat{n} - 2(\hat{n} \cdot \hat{z})\hat{z}$ . Their barycenter is therefore  $\rho_0 = \frac{1}{2}(\mathbf{I} + [\hat{n} - (\hat{n} \cdot \hat{z})\hat{z}] \cdot \vec{\sigma})$ , whose Bloch-vector length is  $|\hat{n} - (\hat{n} \cdot \hat{z})\hat{z}| = |\hat{n} \times \hat{z}|$ . Hence the von Neumann entropy of the barycenter is  $S[\rho_0] = H_1(\frac{1-|\hat{n} \times \hat{z}|}{2})$ , with  $H_1(x) = -x \log x - (1-x) \log(1-x)$ . According to our leaf-level incoherence measure, the most coherent leaves are those with  $|\hat{n} \times \hat{z}| = 1$  (i.e., equatorial spins,  $\hat{n} \cdot \hat{z} = 0$ ), which also maximize the quantum Fisher information with respect to  $H$ .

The first mathematical complications arise in dimension 3 (a single spin-1), where, if we did not restrict the space of states to  $\mathcal{M}_H$ , the leaves would intersect. Here the space of states has real dimension 8 and its representation is trickier. We opt for the standard ex-

pansion in Gell-Mann matrices  $\lambda_j$ ,  $\rho = \frac{1}{3}\mathbf{I} + \frac{1}{2}\vec{n} \cdot \vec{\lambda}$ , where  $n_j = \text{tr}[\rho\lambda_j]$ . Since characterizing the 8-dimensional space is beyond the scope of this work, we consider a diagonal Hamiltonian  $H = \varepsilon_3\lambda_3 + \varepsilon_8\lambda_8$  and focus on a subspace of the foliation characterized by  $\text{tr}[\rho\lambda_j] = 0$  for  $j \in \{2, 4, 5, 6, 7\}$ . Figure 1 depicts the foliation, the amount of incoherence of the leaves, and the corresponding leaf-canonical ensembles. The closure of the leaves are triangles (more generally, simplices) with different size but a common corner. The latter represents an eigenstate of  $H$ , which, in turn, does not belong to  $\mathcal{M}_H$ .

*Leaf typicality hypothesis.* In contrast to the commuting leaf, a generic leaf is not invariant under the time evolution generated by  $H$  but it is transported to a different leaf, while preserving the multiset of energy variances of the associated pure states. Thus, the distribution of energy variances across the pure states defining a leaf is a time-invariant fingerprint of the leaf under the Hamiltonian flow generated by  $H$ . These implicit invariants go beyond the usual conservation laws. Even for a generic Hamiltonian, unitary evolution is highly constrained: it preserves the leaf fingerprint and therefore explores only a thin subset of state space (see also Ref. [34]). In realistic settings (finite resolution, weak noise, or small uncontrolled perturbations), the explored region should be viewed as a “fattened” tube around this constrained set. While any such tube is formally full-dimensional, its effective extent is still organized by the leaf structure and set by the underlying uncertainty scale, which sharply limits the relevant degrees of freedom compared with the full  $(d^2 - 1)$ -dimensional state space.

Infinite-time averaging maps the Hamiltonian orbit to the commuting leaf; at that point, it is widely believed that ergodic principles such as the eigenstate thermalization hypothesis (ETH) apply. This naturally raises the question of whether ETH admits an extension away from the commuting leaf (cf. Ref. [36]); namely, whether for an appropriate class of observables (presumably, local ones) typical states within a given leaf are locally indistinguishable from the corresponding leaf-canonical ensemble (or from its microcanonical counterpart). Focusing on diagonal ETH, one may ask whether for any local observable  $O$  there exists a smooth function  $f_O$  such that for typical eigenstates  $|\Psi_i\rangle$  of  $H_\rho$  with  $E_{\rho,i} \approx E$  (cf. (4))

$$\frac{\langle \Psi_i | \sqrt{\rho} O \sqrt{\rho} | \Psi_i \rangle}{\langle \Psi_i | \rho | \Psi_i \rangle} \sim f_O(E) \quad (8)$$

and the fluctuations within the energy shell vanish as the system size grows. If such a leaf-resolved ETH holds, then the state could be effectively replaced at *any* time by an appropriate effective thermodynamic ensemble, rather than only after long-time dephasing.

We performed a preliminary numerical test of this conjecture on spin- $\frac{1}{2}$  chains of length  $L \leq 12$  (Hilbert-space dimension  $d = 2^L$ ). To avoid degeneracies, we work with

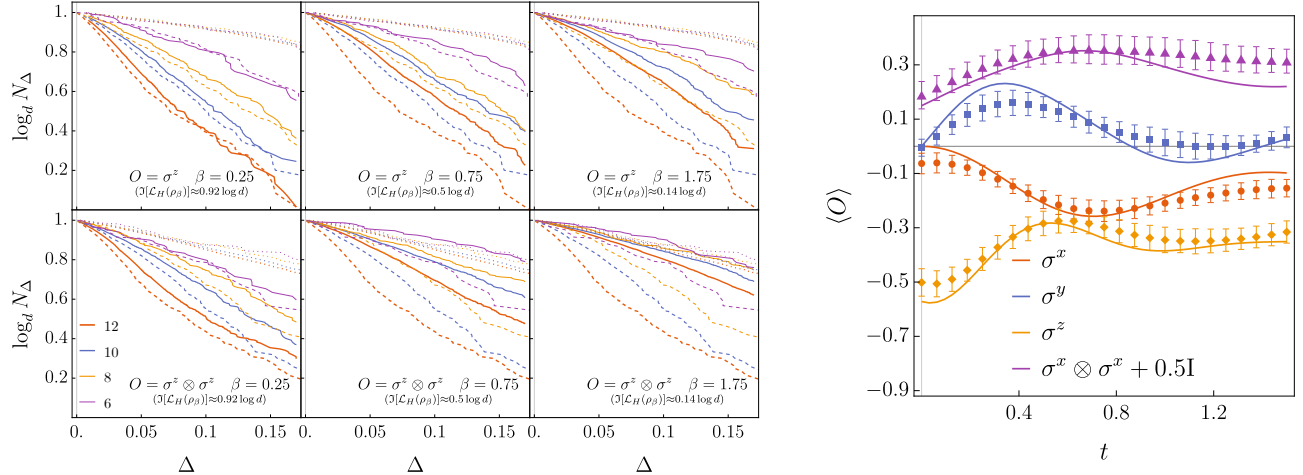


Figure 2. LEFT: Typicality diagnostics (see text) for the local observables  $O \in \{\sigma_\ell^z, \sigma_\ell^z \sigma_{\ell+1}^z\}$  in the min-variance ensemble associated with the nonintegrable Hamiltonian (9) with parameters  $(g, h, D) = (\frac{\sqrt{5}+5}{8}, \frac{\sqrt{5}}{2}, \frac{\pi}{20})$ . The diagnostics are shown for three thermal states  $\rho \propto e^{-\beta H_0}$ , with  $\beta \in \{0.25, 0.75, 1.75\}$ , generated by  $H_0$  of the same form (9) with parameters  $(0, \frac{3}{2}, 0)$  and chain's lengths  $L = \log_2 d \in \{6, 8, 10, 12\}$ . Increasing line thickness corresponds to larger  $L$ . Dashed curves represent the commuting-leaf benchmark ( $\beta = 0$ , i.e.,  $\rho \propto I$ ). For comparison, dotted curves show the commuting-leaf diagnostics for the integrable Hamiltonian  $H_0$ , for which ETH fails [35]. RIGHT: Comparison of the exact time evolution of various operators under Hamiltonian  $H$  (solid lines), starting from  $\rho(0) \propto e^{-\beta H_0}$  with  $\beta = 0.5$  ( $\Im[\mathcal{L}_H(\rho_\beta)] \approx 0.71 \log d$ ), against predictions (markers) from the time evolution of the closest-energy representative state for  $L = 12$ . Error bars denote the 68% confidence interval based on the fraction of outliers in the shell.

a local Hamiltonian without obvious global symmetries

$$H = \sum_\ell^L \sigma_\ell^x \sigma_{\ell+1}^x + g \sigma_\ell^x + h \sigma_\ell^z + D (\sigma_\ell^z \sigma_{\ell+1}^y - \sigma_\ell^y \sigma_{\ell+1}^z), \quad (9)$$

where  $\sigma_\ell^\alpha$  acts as a Pauli matrix on site  $\ell$  and as the identity elsewhere. We choose the couplings so that ETH signatures are already visible at those sizes for all observables supported on one site or on two neighboring sites. We construct  $\rho$  as a thermal state  $\rho = \rho_\beta \propto e^{-\beta H_0}$  of a different Hamiltonian  $H_0$  within the same family; specifically, we take an integrable transverse-field Ising point. To quantify typicality, for each local observable  $O$  we compute the expectation values  $\langle \varphi_i | O | \varphi_i \rangle$  in the optimal ensemble, group states into energy shells with energy  $\sim E$  containing  $O(\sqrt{d})$  consecutive levels, and form the shell average  $f_O(E)$ . We then define  $N_\Delta$  as the total number of eigenstates for which  $|\langle \varphi_i | O | \varphi_i \rangle - f_O(E_{\rho,i})| > \Delta$  and plot  $\log_d N_\Delta$  versus  $\Delta$ . This diagnostic is closely related to large-deviation analyses of the fraction of athermal eigenstates in a microcanonical window [37]. On the commuting leaf, even in its weak form ETH predicts that, at fixed  $\Delta > 0$ , the fraction of outliers vanishes as the system size  $L$  increases [38]. Consequently, the curves sharpen, approaching an increasingly abrupt drop that tends towards a vertical line. Any different asymptotic trend would indicate the presence of an exponentially large set of atypical eigenstates whose local expectation values remain distinct from the thermal ones.

Figure 2-left illustrates the behavior of two representative observables at three inverse temperatures (w.r.t.  $H_0$ ) away from the commuting leaf (w.r.t.  $H$ ). The data fairly support the hypothesis of leaf typicality. However, as the energy incoherence  $\Im[\mathcal{L}_H(\rho_\beta)]$  decreases, the distribution of expectation values broadens, and the convergence to the ETH-like result appears to slow down. Figure 2-right illustrates the dynamical content of leaf typicality: for local observables, the exact evolution are reproduced by evolving a representative (pure) state drawn from the optimal ensemble, even when the evolving density matrix is highly mixed. While representative-state ideas are not new [39], even out of equilibrium [40–42], leaf typicality stands out by providing a state-resolved representative description, rather than a probabilistic consequence of concentration-of-measure typicality. We refer the reader to the Supplemental Material for additional tests [43].

*Discussion.* We have introduced a foliation of the state space of a quantum system based on the minimization of coherent energy fluctuations. This framework enables a generalization of thermodynamic ensembles beyond equilibrium, offering a comparably effective distillation of microscopic complexity into macroscopic properties. In particular, we proposed a “leaf typicality” hypothesis, which suggests a scenario where leaves replace states as the fundamental objects of description. The foliation also naturally induces a quantitative notion of quantum (in)coherence with respect to the Hamiltonian,

providing a new tool for characterizing nonequilibrium states. To keep the discussion focused, we deliberately restricted our analysis to the nondegenerate case for  $H_\rho$ . This choice excludes situations where  $H_\rho$  has reduced rank and admits inequivalent extensions, corresponding to intersections between distinct leaves. We made this simplification both for clarity and because we anticipate that the boundary structure of the leaves (their faces and intersections) will exhibit distinctive physical features that warrant a separate study.

A number of open questions remain, beginning with identifying the most natural subspace for accommodating the leaf-typicality hypothesis. Additionally, we did not address the dynamics of relaxation towards the commuting leaf. In that context, the foliation that we introduced suggests an appealing route to open-system dynamics: one may seek nonunitary evolutions that act compatibly with the foliation by mapping leaves into leaves. Within such a framework, dephasing could be modeled as the net effect of weak noise that drives states towards reduced energy-basis coherence, plausibly aided by an entropic bias (regions of higher incoherence occupy a larger volume in state space). A natural setting for such a mechanism is provided by standard subsystem maps. Indeed, the partial trace sends a leaf of the full system to the convex hull of the reduced density matrices obtained from the leaf's pure-state ensemble, which is generically not a single leaf of the subsystem. On the other hand, if leaf typicality holds, local observables would still depend only on the leaf and the total energy. This raises the possibility of an effective description in which the convex hull above can be reduced to a single leaf of an emergent foliation on subsystem state space, with entropic bias playing a key role in shaping that foliation. Finally, we have not examined the implications of conservation laws, which are particularly important for generalizing the framework to integrable systems.

I thank Florent Ferro and Luca Capizzi for discussions.

---

\* [maurizio.fagotti@universite-paris-saclay.fr](mailto:maurizio.fagotti@universite-paris-saclay.fr)

- [1] L. Boltzmann, Further Studies on the Thermal Equilibrium of Gas Molecules, in *The Kinetic Theory of Gases: An Anthology of Classic Papers with Historical Commentary*, History of Modern Physical Sciences, Vol. 1, edited by S. G. Brush (World Scientific, 2003) pp. 262–349, english translation of Boltzmann (1872) *Weitere Studien über das Wärmegeleichgewicht unter Gasmolekülen*.
- [2] A. Polkovnikov, K. Sengupta, A. Silva, and M. Vengalattore, Colloquium: Nonequilibrium dynamics of closed interacting quantum systems, *Rev. Mod. Phys.* **83**, 863 (2011).
- [3] J. Eisert, M. Friesdorf, and C. Gogolin, Quantum many-body systems out of equilibrium, *Nature Physics* **11**, 124 (2015).
- [4] M. Rigol, V. Dunjko, V. Yurovsky, and M. Olshani, Relaxation in a Completely Integrable Many-Body Quantum System: An Ab Initio Study of the Dynamics of the Highly Excited States of 1D Lattice Hard-Core Bosons, *Phys. Rev. Lett.* **98**, 050405 (2007).
- [5] F. H. L. Essler and M. Fagotti, Quench dynamics and relaxation in isolated integrable quantum spin chains, *Journal of Statistical Mechanics: Theory and Experiment* **2016**, 064002 (2016).
- [6] E. B. Davies and J. T. Lewis, An operational approach to quantum probability, *Communications in Mathematical Physics* **17**, 239 (1970).
- [7] S. L. Braunstein and C. M. Caves, Statistical distance and the geometry of quantum states, *Phys. Rev. Lett.* **72**, 3439 (1994).
- [8] M. G. A. Paris, Quantum estimation for quantum technology, *International Journal of Quantum Information* **7**, 125 (2009).
- [9] T. Barthel and U. Schollwöck, Dephasing and the Steady State in Quantum Many-Particle Systems, *Phys. Rev. Lett.* **100**, 100601 (2008).
- [10] P. Reimann, Foundation of Statistical Mechanics under Experimentally Realistic Conditions, *Phys. Rev. Lett.* **101**, 190403 (2008).
- [11] N. Linden, S. Popescu, A. J. Short, and A. Winter, Quantum mechanical evolution towards thermal equilibrium, *Phys. Rev. E* **79**, 061103 (2009).
- [12] T. R. de Oliveira, C. Charalambous, D. Jonathan, M. Lewenstein, and A. Riera, Equilibration time scales in closed many-body quantum systems, *New Journal of Physics* **20**, 033032 (2018).
- [13] J. M. Deutsch, Quantum statistical mechanics in a closed system, *Phys. Rev. A* **43**, 2046 (1991).
- [14] M. Srednicki, Chaos and quantum thermalization, *Phys. Rev. E* **50**, 888 (1994).
- [15] M. Rigol, V. Dunjko, and M. Olshanii, Thermalization and its mechanism for generic isolated quantum systems, *Nature* **452**, 854 (2008).
- [16] L. D'Alessio, Y. Kafri, A. Polkovnikov, and M. Rigol, From quantum chaos and eigenstate thermalization to statistical mechanics and thermodynamics, *Advances in Physics* **65**, 239 (2016).
- [17] T. Kuwahara and K. Saito, Eigenstate Thermalization from the Clustering Property of Correlation, *Phys. Rev. Lett.* **124**, 200604 (2020).
- [18] R. Lima, Equivalence of ensembles in quantum lattice systems: States, *Communications in Mathematical Physics* **24**, 180 (1972).
- [19] H. Tasaki, On the Local Equivalence Between the Canonical and the Microcanonical Ensembles for Quantum Spin Systems, *Journal of Statistical Physics* **172**, 905 (2018).
- [20] T. Kuwahara and K. Saito, Gaussian concentration bound and ensemble equivalence in generic quantum many-body systems including long-range interactions, *Annals of Physics* **421**, 168278 (2020).
- [21] F. G. S. L. Brandão and M. Cramer, Equivalence of Statistical Mechanical Ensembles for Non-Critical Quantum Systems (2015), [arXiv:1502.03263 \[quant-ph\]](https://arxiv.org/abs/1502.03263).
- [22] G. Tóth and D. Petz, Extremal properties of the variance and the quantum Fisher information, *Phys. Rev. A* **87**, 032324 (2013).
- [23] S. Yu, Quantum Fisher Information as the Convex Roof of Variance, [arXiv:1302.5311 \[quant-ph\]](https://arxiv.org/abs/1302.5311) (2013).
- [24] If  $\{|\varphi_i\rangle\}$  satisfy (2), then  $F_Q(\rho; H) = 4 \sum_i p_i \text{Var}_{\varphi_i}(H)$ .
- [25] A. Uhlmann, Roofs and Convexity, *Entropy* **12**, 1799

(2010).

[26] B. Regula, Convex geometry of quantum resource quantification, *Journal of Physics A: Mathematical and Theoretical* **51**, 045303 (2017).

[27] E. T. Jaynes, Information Theory and Statistical Mechanics, *Phys. Rev.* **106**, 620 (1957).

[28] A. Streltsov, G. Adesso, and M. B. Plenio, Colloquium: Quantum coherence as a resource, *Rev. Mod. Phys.* **89**, 041003 (2017).

[29] M. Lostaglio, D. Jennings, and T. Rudolph, Description of quantum coherence in thermodynamic processes requires constraints beyond free energy, *Nature Communications* **6**, 6383 (2015).

[30] T. Baumgratz, M. Cramer, and M. B. Plenio, Quantifying Coherence, *Phys. Rev. Lett.* **113**, 140401 (2014).

[31] C. A. Fuchs and M. Sasaki, Squeezing Quantum Information through a Classical Channel: Measuring the “Quantumness” of a Set of Quantum States, *Quantum Information & Computation* **3**, 377 (2003).

[32] Y. Sun, S. Luo, and X. Lei, Quantumness of ensemble via coherence of Gram matrix, *EPL (Europhysics Letters)* **134**, 30003 (2021).

[33] T. Theurer, N. Killoran, D. Egloff, and M. B. Plenio, Resource Theory of Superposition, *Physical Review Letters* **119**, 230401 (2017).

[34] M. Fagotti, On the size of the space spanned by a nonequilibrium state in a quantum spin lattice system, *SciPost Phys.* **6**, 059 (2019).

[35] R. Steinigeweg, J. Herbrych, and P. Prelovšek, Eigenstate thermalization within isolated spin-chain systems, *Phys. Rev. E* **87**, 012118 (2013).

[36] L. Foini, A. Dymarsky, and S. Pappalardi, Out-of-equilibrium eigenstate thermalization hypothesis, *SciPost Phys.* **18**, 136 (2025).

[37] T. Yoshizawa, E. Iyoda, and T. Sagawa, Numerical Large Deviation Analysis of the Eigenstate Thermalization Hypothesis, *Phys. Rev. Lett.* **120**, 200604 (2018).

[38] H. Kim, T. N. Ikeda, and D. A. Huse, Testing whether all eigenstates obey the eigenstate thermalization hypothesis, *Phys. Rev. E* **90**, 052105 (2014).

[39] S. Sugiura and A. Shimizu, Canonical Thermal Pure Quantum State, *Phys. Rev. Lett.* **111**, 010401 (2013).

[40] C. Bartsch and J. Gemmer, Dynamical Typicality of Quantum Expectation Values, *Phys. Rev. Lett.* **102**, 110403 (2009).

[41] J.-S. Caux and F. H. L. Essler, Time Evolution of Local Observables After Quenching to an Integrable Model, *Phys. Rev. Lett.* **110**, 257203 (2013).

[42] J.-S. Caux, The Quench Action, *Journal of Statistical Mechanics: Theory and Experiment* **2016**, 064006 (2016).

[43] See Supplemental Material.

---

## SUPPLEMENTAL MATERIAL

### *Quantum-Coherent Thermodynamics: Leaf Typicality via Minimum-Variance Foliation*

#### LEAF TYPICALITY: ADDITIONAL NUMERICAL TESTS

In the main text we presented data supporting the leaf-typicality hypothesis for two representative observables,  $\sigma_\ell^z$  and  $\sigma_\ell^z \sigma_{\ell+1}^z$ . To address natural concerns about the generality of this test, we report here the corresponding results for the complete set of local observables supported on one site and on two neighboring sites. To avoid reproducing the same parameter set, we also modify the Hamiltonian  $H_0$  defining the thermal state. While the main text used a transverse-field Ising point in the “paramagnetic” regime, here we consider an Ising point in the “ferromagnetic” regime (the quotation marks emphasize that our states are at finite temperature; the labels “paramagnetic” and “ferromagnetic” refer instead to the zero-temperature phase diagram of  $H_0$ ). The data are shown in Figures S1, S2 and S3, which differ only in the temperature of the state. As commented in the main text, the data seem to be consistent with leaf typicality, but the convergence to the ETH-like result appears to slow down as the energy incoherence  $\Im[\mathcal{L}_H(\rho_\beta)]$  decreases.

We also demonstrate the breakdown of leaf typicality for integrable dynamics. To this end, we interchange the roles of  $H$  and  $H_0$ : we prepare a thermal state of  $H$  and study the foliation induced by the integrable Hamiltonian  $H_0$ . Figure S4 shows that the typicality diagnostic no longer sharpens with system size, consistent with the presence of additional conserved quantities.

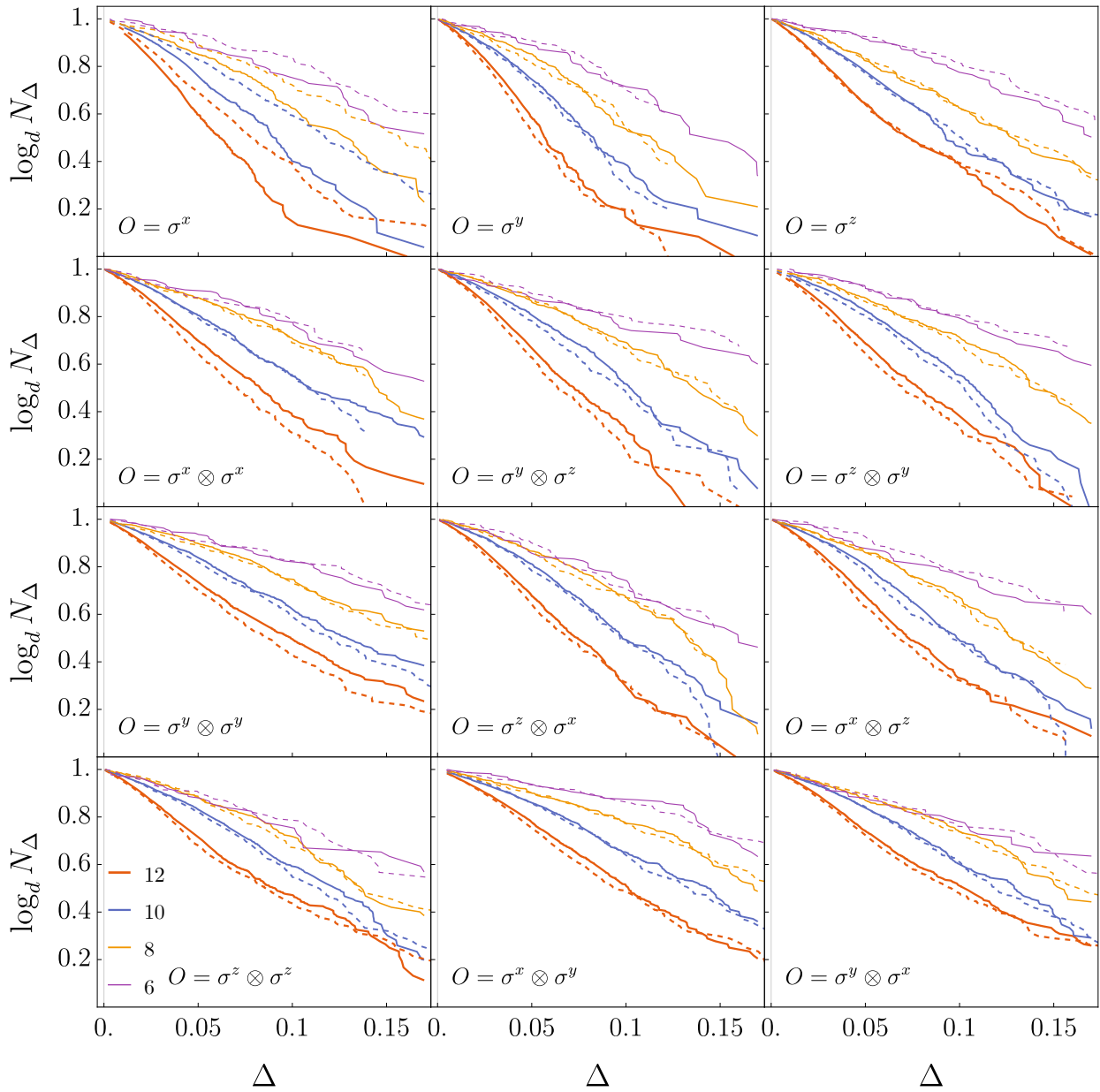


Figure S1. Typicality diagnostics (see main text) for all local observables with support on 1 or 2 neighboring sites in the min-variance ensemble associated with the nonintegrable Hamiltonian (9) with parameters  $(g, h, D) = (\frac{\sqrt{5}+5}{8}, \frac{\sqrt{5}}{2}, \frac{\pi}{20})$ . The state is thermal,  $\rho \propto e^{-\beta H_0}$ , with inverse temperature  $\beta = 0.25$  and  $H_0$  has the same form (9) with parameters  $(0, \frac{1}{2}, 0)$ . The considered chain's lengths are  $L = \log_2 d \in \{6, 8, 10, 12\}$ . Increasing line thickness corresponds to larger  $L$ . Dashed curves represent the commuting-leaf benchmark ( $\beta = 0$ , i.e.,  $\rho \propto \mathbf{I}$ ). The energy incoherence is  $\Im[\mathcal{L}_H(\rho_\beta)] \approx 0.97 \log d$ .

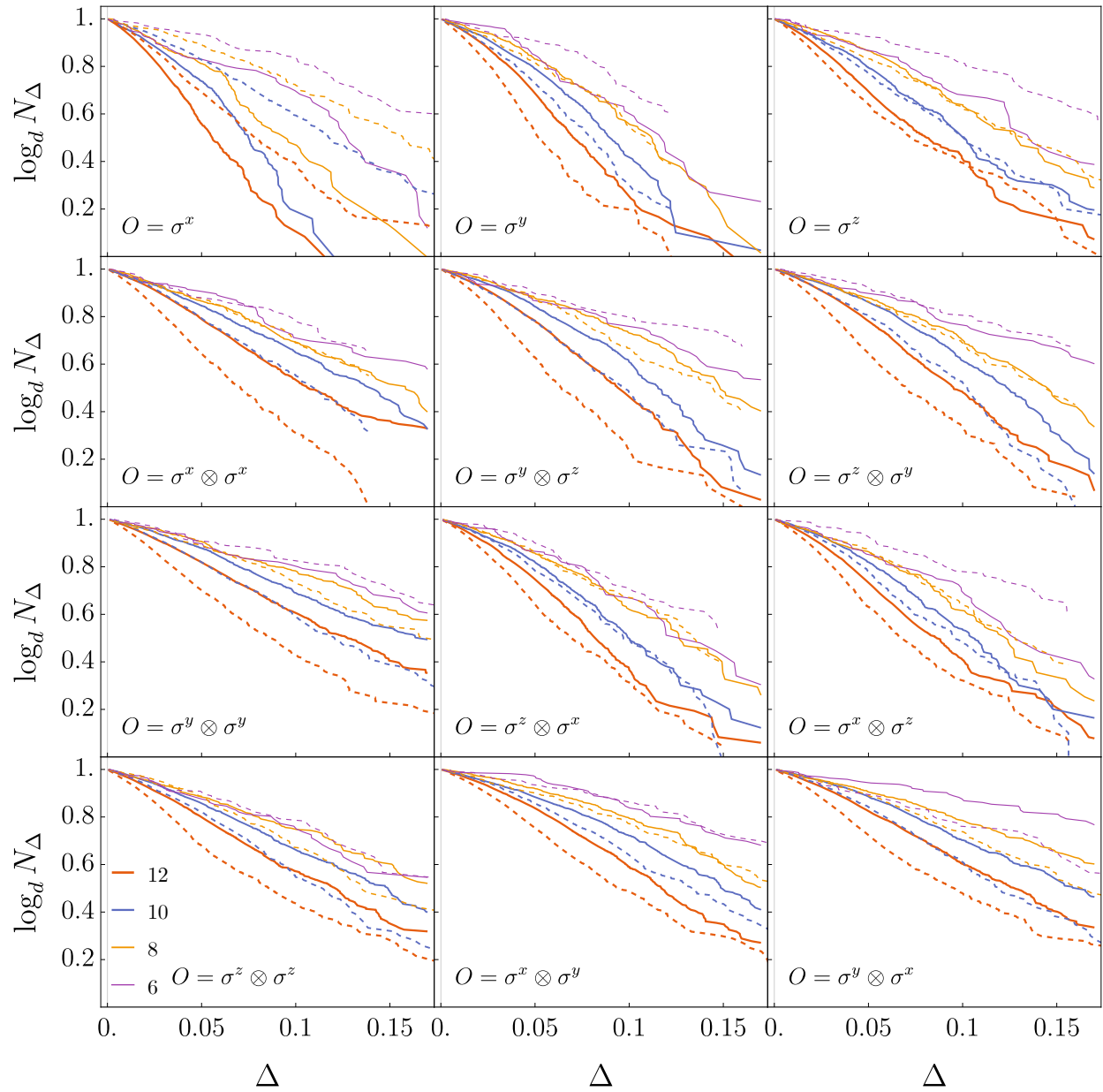


Figure S2. The same as in Fig. S1 with  $\beta = 0.75$  (the energy incoherence is  $\Im[\mathcal{L}_H(\rho_\beta)] \approx 0.76 \log d$ ).

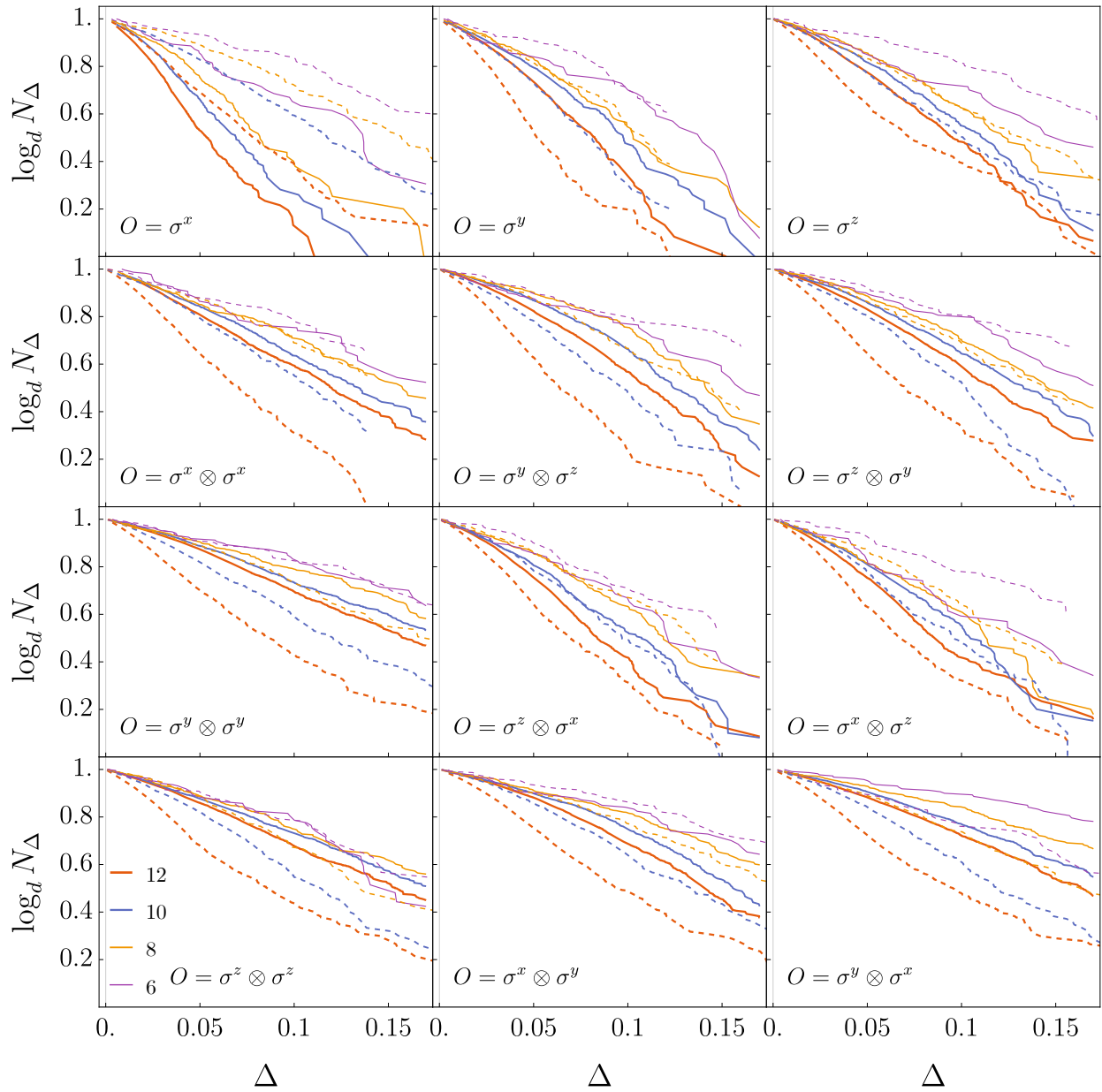


Figure S3. The same as in Fig. S1 with  $\beta = 1.75$  (the energy incoherence is  $\Im[\mathcal{L}_H(\rho_\beta)] \approx 0.24 \log d$ ).

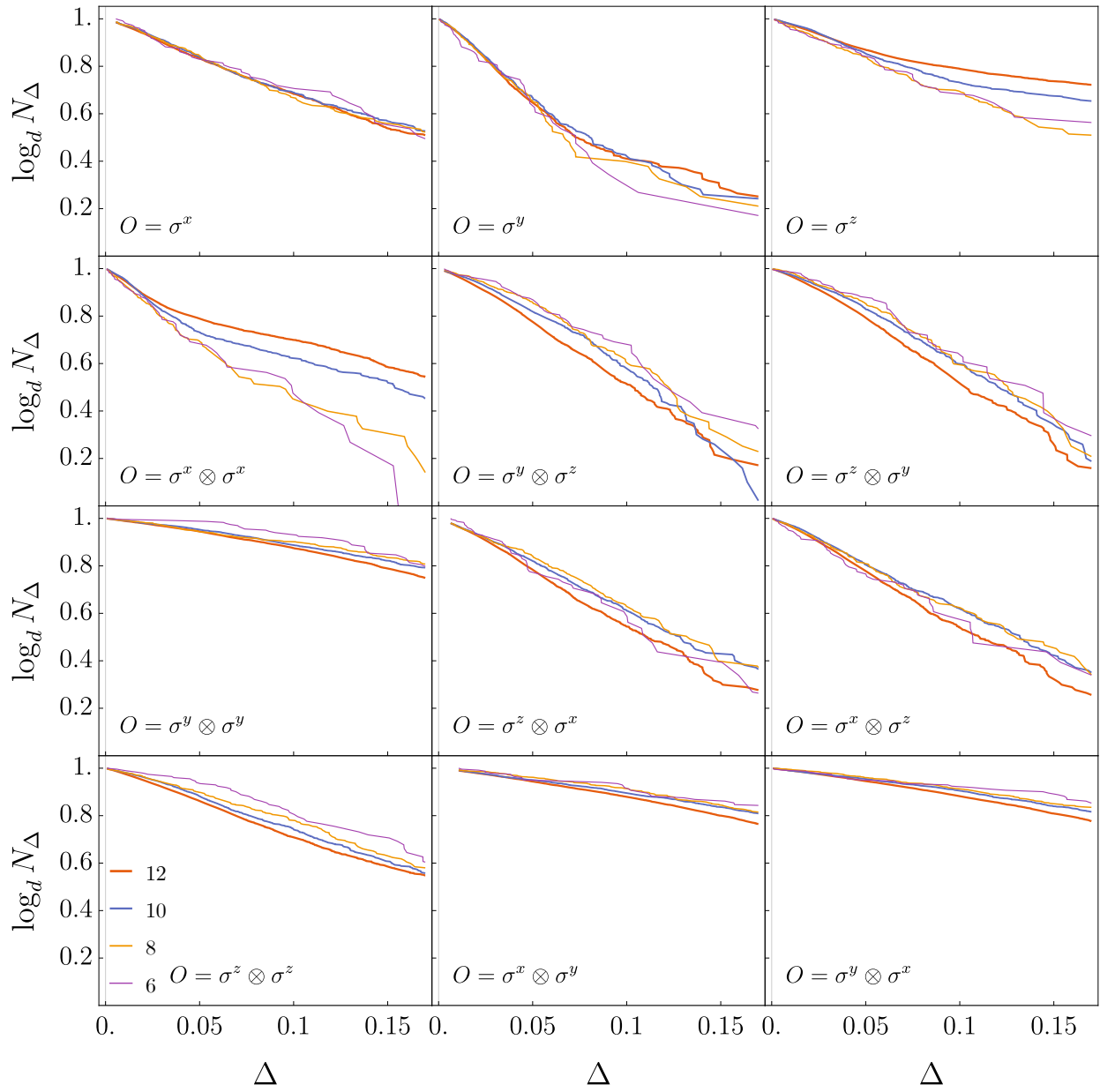


Figure S4. The same as in Fig. S1 with  $\beta = 0.25$  but  $H_0$  and  $H$  interchanged ( $\Im[\mathcal{L}_{H_0}(\rho_\beta)] \approx 0.92 \log d$ ).